

**SUPPLEMENTAL INFORMATION:**

**Intervention with citrus flavonoids reverses obesity, and improves metabolic syndrome and atherosclerosis in obese *Ldlr*<sup>-/-</sup> mice**

Amy C. Burke<sup>1,2</sup>, Brian G. Sutherland<sup>1</sup>, Dawn E. Telford<sup>1,3</sup>, Marisa R. Morrow<sup>1</sup>, Cynthia G. Sawyez<sup>1,3</sup>, Jane Y. Edwards<sup>1,3</sup>, Maria Drangova<sup>4</sup>, Murray W. Huff<sup>1,2,3,5</sup>

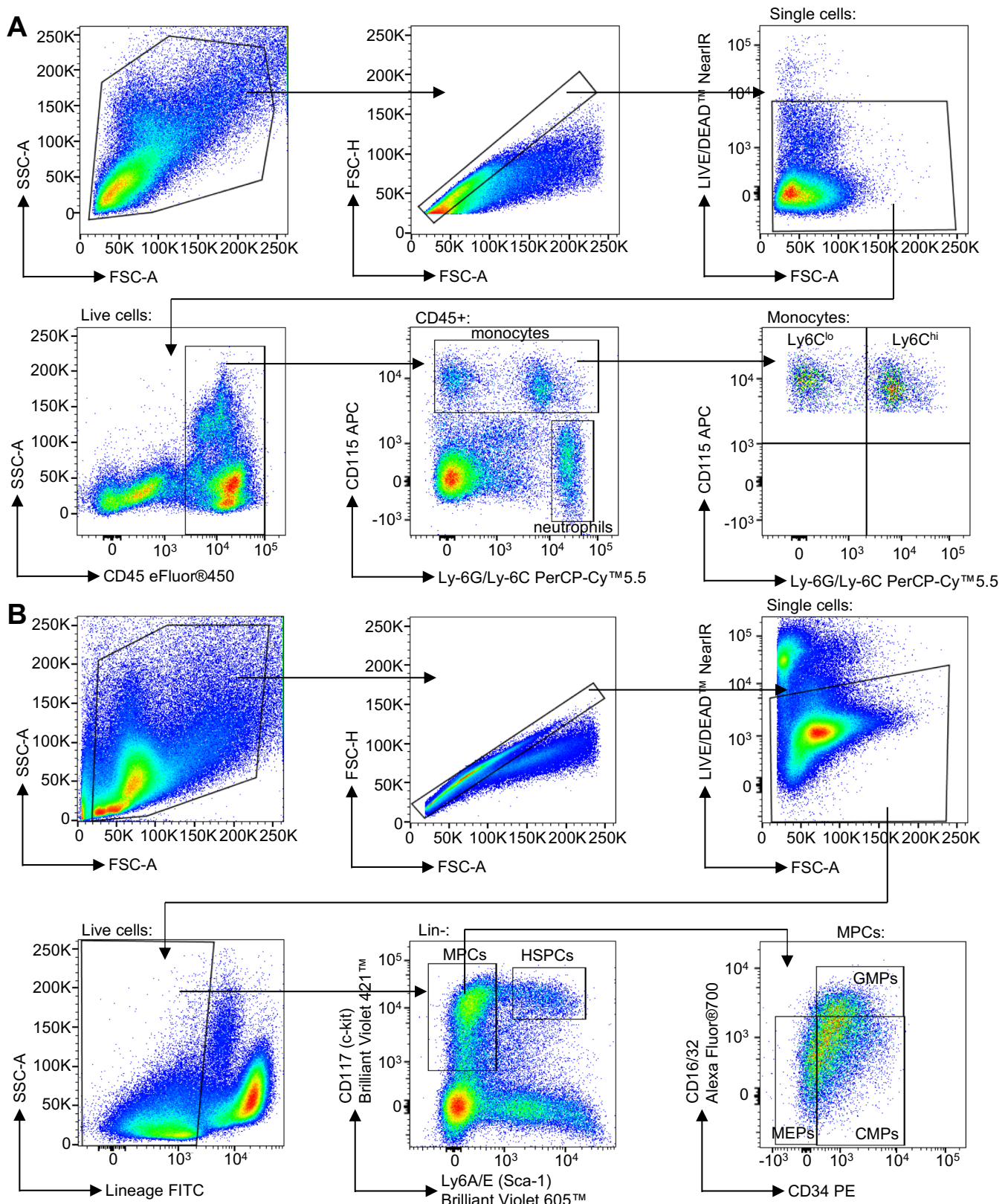
<sup>1</sup>Molecular Medicine, Robarts Research Institute, <sup>2</sup>Departments of Biochemistry and <sup>3</sup>Medicine,

<sup>4</sup>Imaging Research Laboratories, Robarts Research Institute, The University of Western Ontario,

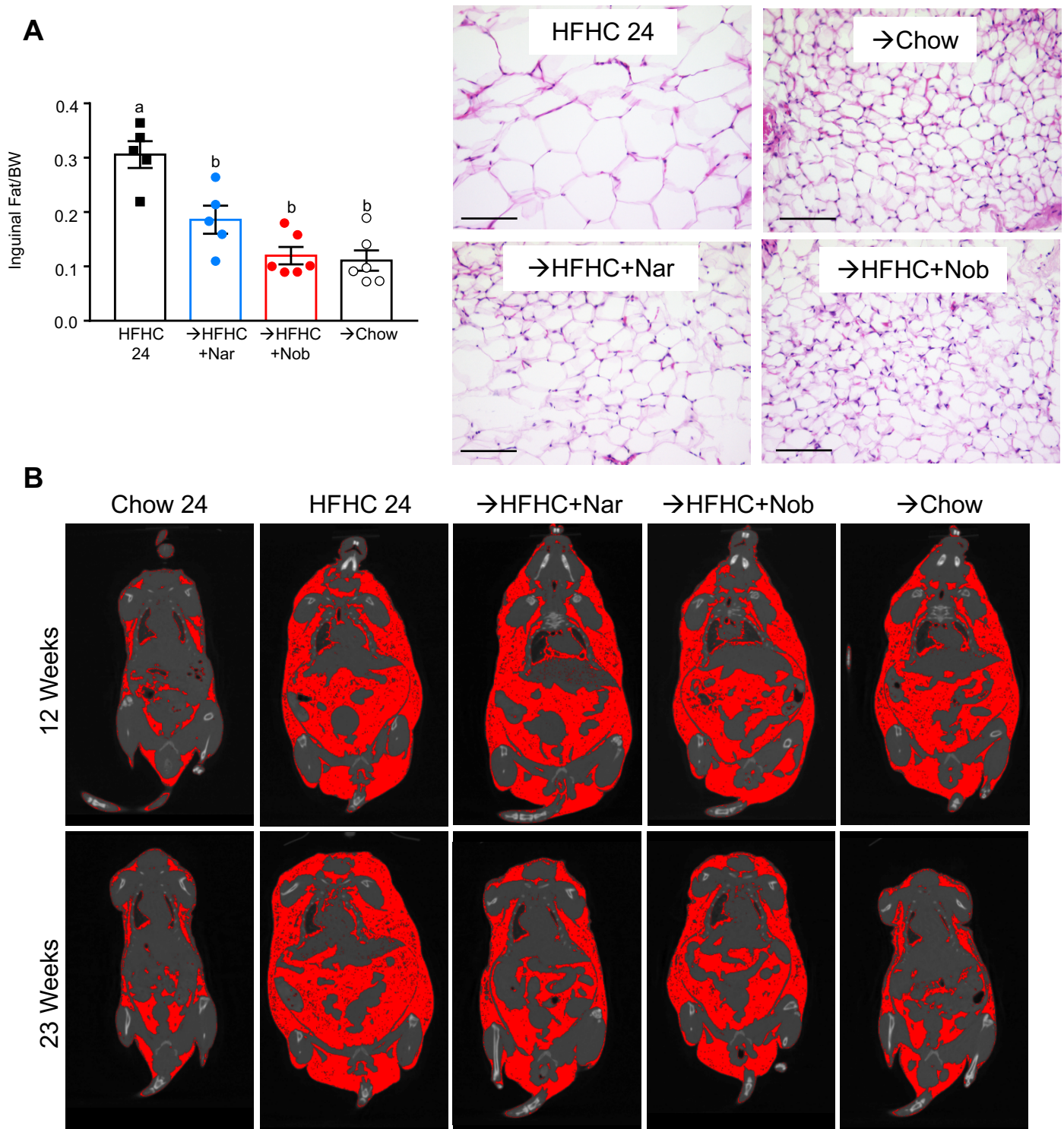
1151 Richmond St N., London, Ontario, Canada N6A 5B7

Supplementary Table S1. Antibodies Used for Flow Cytometry.

Antibody	Isotype-Matched Control	Dilution	Source	Catalogue No.
PerCP-Cy <sup>TM</sup> 5.5 Rat Anti-Mouse Ly-6G and Ly-6C	Rat IgG2b, $\kappa$	1/200	BD Biosciences	552093
eFluor <sup>®</sup> 450 Anti-Mouse CD45	Rat IgG2b, $\kappa$	1/40	Affymetrix eBioscience	48-0451
FITC Mouse Hematopoietic Lineage Cocktail <ul style="list-style-type: none"> <li>• Anti-mouse CD3 (17A2)</li> <li>• Anti-mouse CD45R (B220)(RA3-6B2)</li> <li>• Anti-mouse CD11b (M1/70)</li> <li>• Anti-mouse TER-119</li> <li>• Anti-mouse Ly-G6 (Gr-1) (RB6-8C5)</li> </ul>	N/A	20 $\mu$ l	Affymetrix eBioscience	22-7770
Brilliant Violet 421 <sup>TM</sup> Anti-mouse CD117 (c-Kit)	Rat IgG2b, $\kappa$	1/40	Biolegend	105828
Brilliant Violet 605 <sup>TM</sup> anti-mouse Ly-6A/E (Sca-1)	Rat IgG2a, $\kappa$	1/40	Biolegend	108133
Alexa Fluor <sup>®</sup> 700 Anti-mouse CD16/32	Rat IgG2a, $\lambda$	1/80	Affymetrix, eBioscience	56-0161
APC Anti-mouse CD115 (c-fms)	Rat IgG2a, $\kappa$	1/200	Affymetrix eBioscience	17-1152
PE Anti-mouse CD34	Armenian Hamster IgG	1/80	Biolegend	128610
LIVE/DEAD <sup>®</sup> Fixable Dead Cell Near-IR Stain Kits		1 $\mu$ l	Invitrogen	L10119

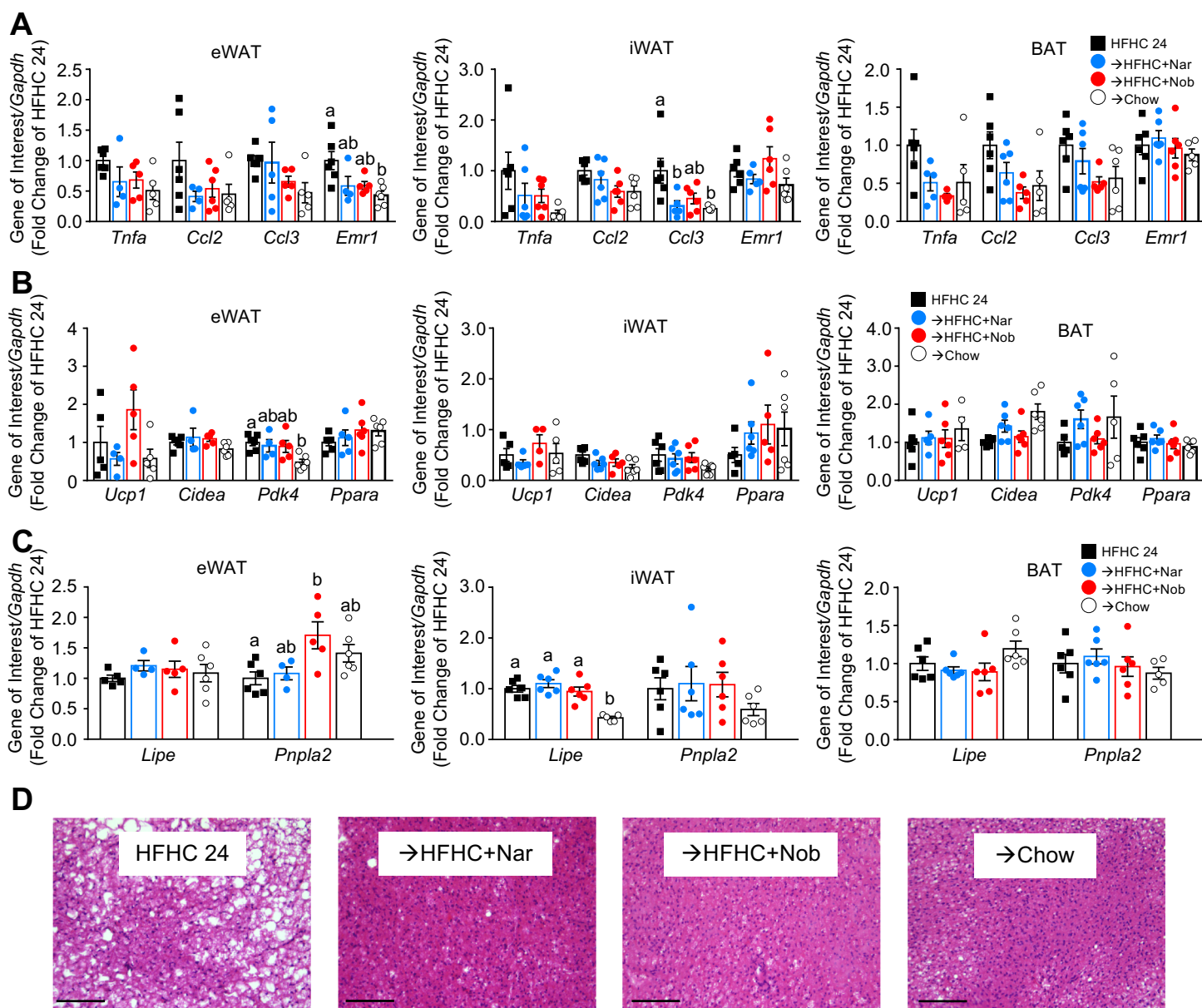


**Supplementary Figure S1.** Gating Strategy for Peripheral Blood Mononuclear Cells and Bone Marrow Progenitor Populations. *Ldlr*<sup>-/-</sup> mice were fed a HFHC diet for 12 weeks. Subsequently the same mice were treated with flavonoids added to the HFHC diet for an additional 12 weeks. A; Gating strategy for blood monocytes and neutrophils. B; Gating strategy for bone marrow progenitor populations.

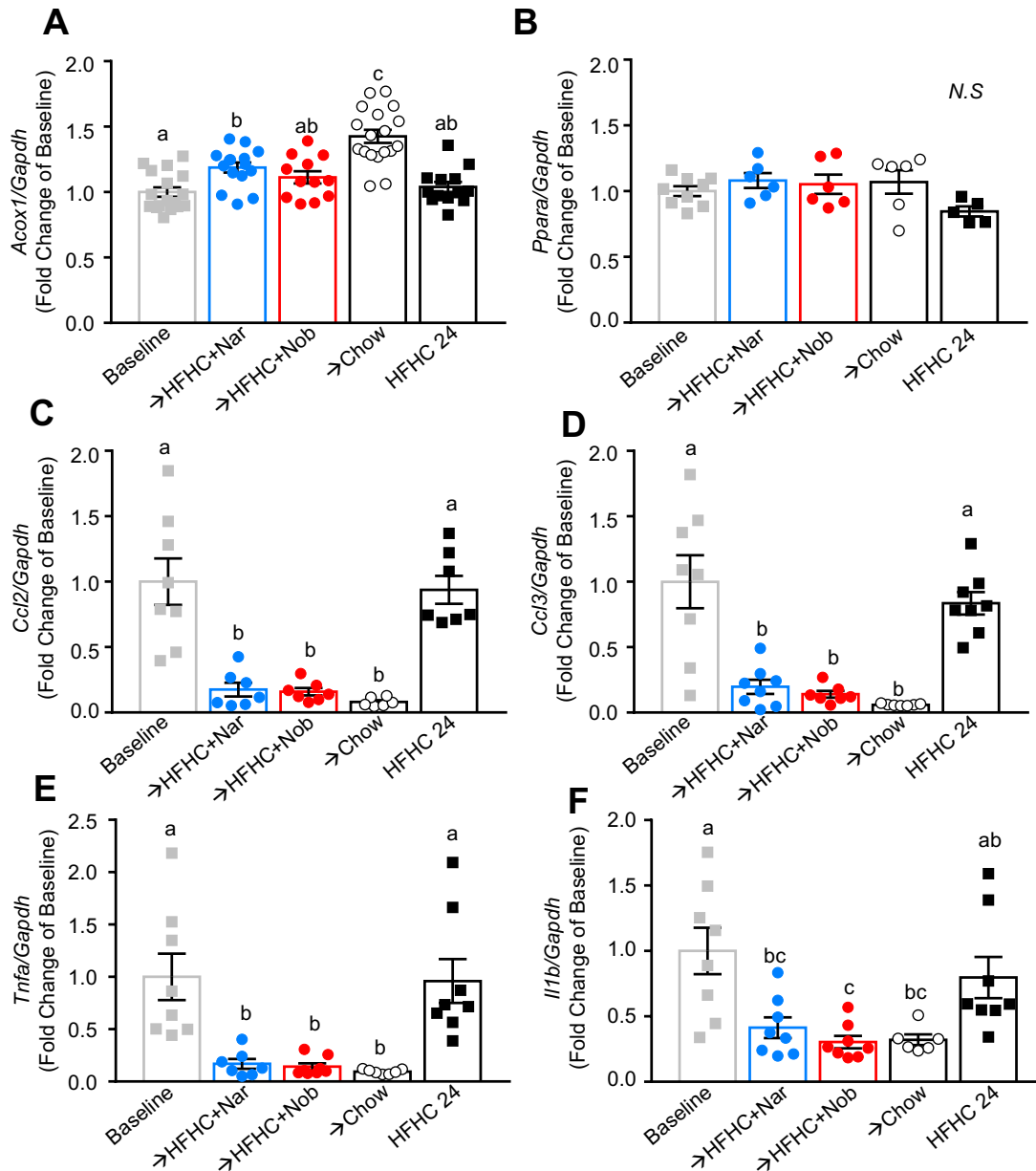


**Supplementary Figure S2.** Intervention with Citrus Flavonoids Reduces Adiposity. *Ldlr*<sup>-/-</sup> mice were fed a HFHC diet for 12 weeks. Subsequently, the same mice were treated with flavonoids added to the HFHC diet for an additional 12 weeks. A; Inguinal white adipose tissue weight as a proportion of total body weight (n=6-8/group) and representative sections of inguinal adipose tissue stained with hematoxylin and eosin. Scale bar is 100µm. B; Representative microCT images of the same mice at baseline (12 weeks HFHC induction) and following intervention (23 weeks); adipose tissue is highlighted in red. Data represent the mean±SEM. Different letters are statistically different by ANOVA with post-hoc Tukey test ( $P<0.05$ ).

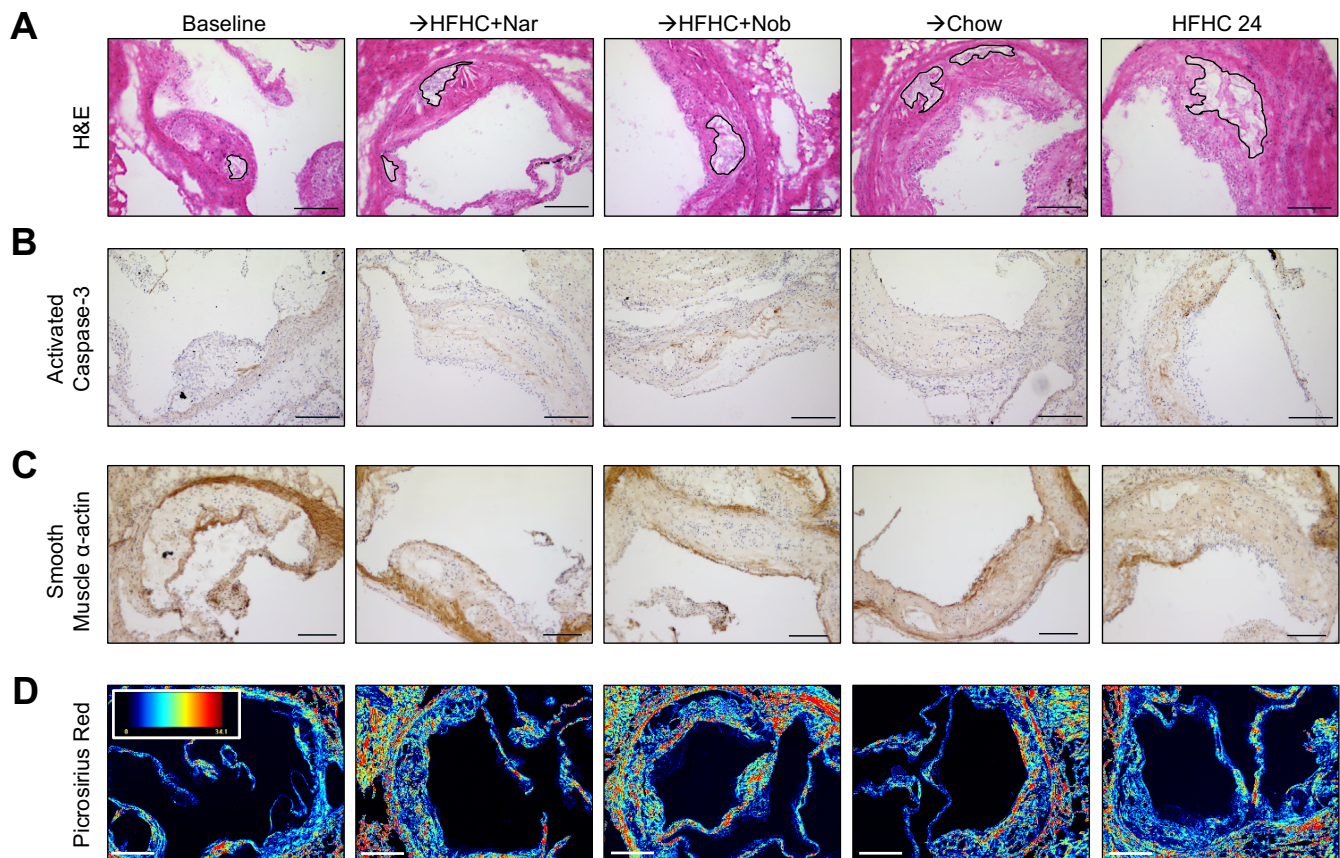




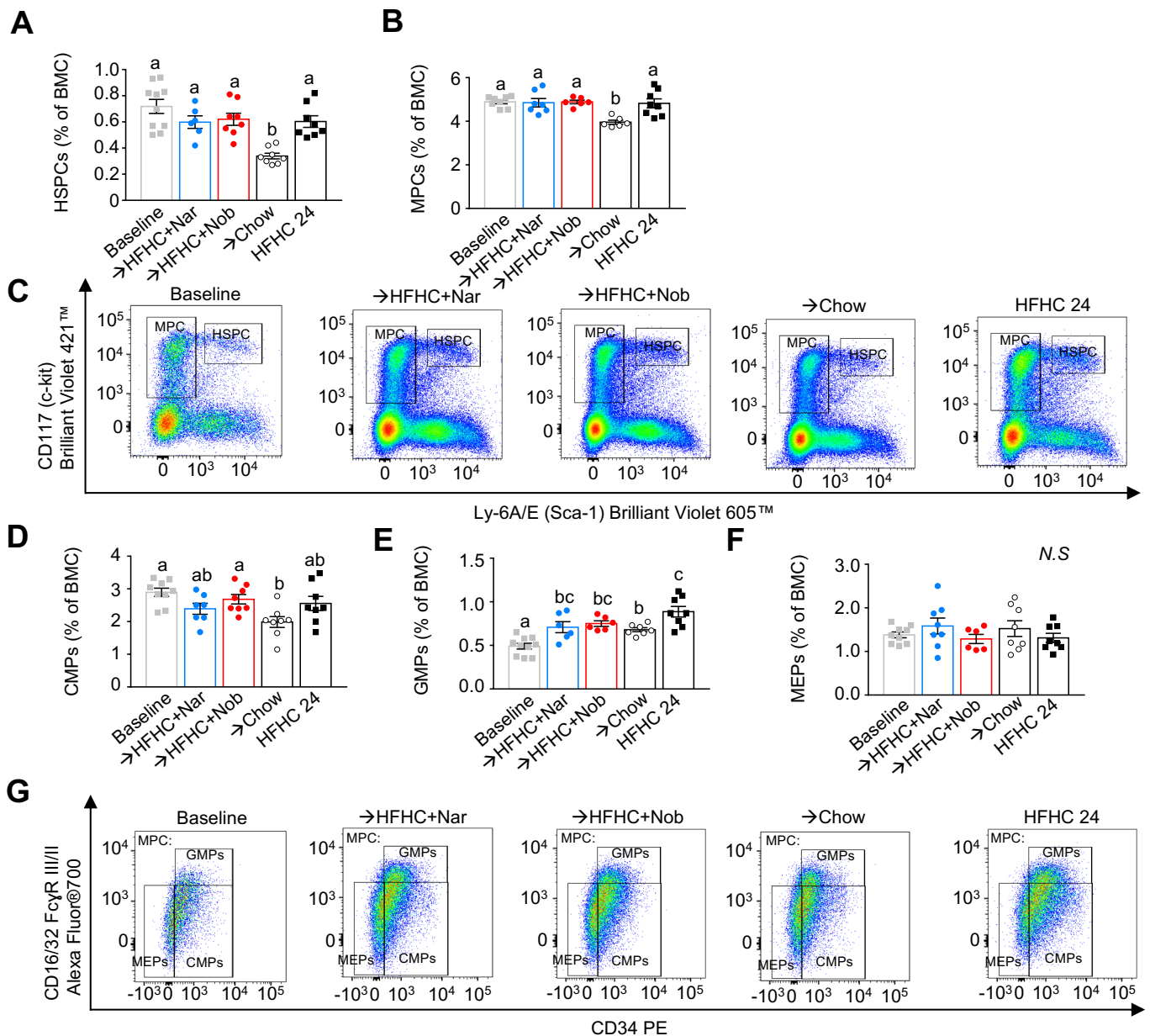
**Supplementary Figure S3.** Intervention with Citrus Flavonoids Modestly Attenuates Adipose Tissue Inflammation, with no Effect on Browning or Lipolysis Gene Expression. *Ldlr*<sup>-/-</sup> mice were fed a HFHC diet for 12 weeks. Subsequently the same mice were treated with flavonoids added to the HFHC diet for an additional 12 weeks. A; Expression of inflammatory genes, *Tnfa*, *Ccl2*, *Ccl3* and macrophage specific gene, *Emr1*, in epididymal white adipose tissue, inguinal white adipose tissue and brown adipose tissue (n=6/group). B; Expression of browning genes, *Ucp1*, *Cidea*, *Pdk4*, *Ppara*, in epididymal white adipose tissue, inguinal white adipose tissue and brown adipose tissue (n=6/group). C; Expression of lipolysis genes, *Lipe*, and *Pnpla2*, in epididymal white adipose tissue, inguinal white adipose tissue and brown adipose tissue (n=6/group). D; Representative sections of brown adipose tissue stained with hematoxylin and eosin. Scale bar is 100  $\mu$ m. Data represent the mean $\pm$ SEM. Different letters are statistically different by ANOVA with post-hoc Tukey test ( $P < 0.05$ ).



**Supplementary Figure S4.** Flavonoid Intervention Reduces Hepatic Inflammation. *Ldlr*<sup>-/-</sup> mice were fed a HFHC diet for 12 weeks. Subsequently the same mice were treated with flavonoids added to the HFHC diet for an additional 12 weeks. A; Hepatic expression of A; *Acox1*, B; *Ppara* C; *Ccl2*, D; *Ccl3*, E; *Tnfa*, and F; *Il1b* normalized to baseline (n=6-12/group). Data represent the mean±SEM. Different letters are statistically different by ANOVA with post-hoc Tukey test ( $P<0.05$ ). N.S. indicates no significant difference.



**Supplementary Figure S5.** Representative Images for Histological Analysis of Aortic Sinus Atherosclerotic Lesions. *Ldlr*<sup>-/-</sup> mice were fed a HFHC diet for 12 weeks. Subsequently the same mice were treated with flavonoids added to the HFHC diet for an additional 12 weeks. A; Hematoxylin and eosin stained sections of the aortic sinus with outlined necrotic core area ( $>3000\mu\text{m}^2$ ). Scale bar is 200  $\mu\text{m}$ . B; Aortic sinus sections immunostained for cleaved caspase-3, a marker of cell apoptosis, and counterstained with hematoxylin. Scale bar is 200  $\mu\text{m}$ . C; Aortic sinus sections immunostained for smooth muscle  $\alpha$ -actin and counterstained with hematoxylin. Scale bar is 200  $\mu\text{m}$ . D; Aortic sinus sections stained with picrosirius red and imaged using circular polarization microscopy. Scale bar is 250  $\mu\text{m}$ . Color encoding of light retardation (nm) is depicted in the gradient map (blue: low; red: high). Quantitation appears in Figure 7.



**Supplementary Figure S6.** Intervention with Citrus Flavonoids Modestly Reduces Bone Marrow Progenitors. *Ldlr*<sup>-/-</sup> mice were fed a HFHC diet for 12 weeks. Subsequently the same mice were treated with flavonoids added to the HFHC diet for an additional 12 weeks. Bone marrow cells were isolated and stained for markers of progenitor populations. A; Percent of bone marrow cells that were hematopoietic stem and progenitors (HSPC) ( $Lin^{-}$ ,  $Sca-1^{+}$ ,  $ckit^{+}$ ) ( $n=8-10$ /group). B; Percent of bone marrow cells that were myeloid progenitors (MPC) ( $Lin^{-}$ ,  $Sca-1^{-}$ ,  $ckit^{+}$ ) ( $n=8-10$ /group). C; Representative flow cytometric pseudocolor plots show HSPCs and MPCs. D; Percent of bone marrow cells that were common myeloid progenitors (CMPs) ( $Lin^{-}$ ,  $Sca-1^{-}$ ,  $ckit^{+}$ ,  $CD16/32^{-}$ ,  $CD34^{+}$ ) ( $n=8-10$ /group). E; Percent of bone marrow cells that were granulocyte and macrophage progenitors (GMPs) ( $Lin^{-}$ ,  $Sca-1^{-}$ ,  $ckit^{+}$ ,  $CD16/32^{+}$ ,  $CD34^{+}$ ) ( $n=8-10$ /group). F; Percent of bone marrow cells that were megakaryocyte and erythrocyte progenitors (MEPs) ( $Lin^{-}$ ,  $Sca-1^{-}$ ,  $ckit^{+}$ ,  $CD16/32^{-}$ ,  $CD34^{-}$ ) ( $n=8-10$ /group). G; Representative flow cytometric pseudocolor plots show CMPs, GMPs and MEPs. Data represent the mean $\pm$ SEM. Different letters are statistically different by ANOVA with post-hoc Tukey test ( $P<0.05$ ). N.S. indicates no significant difference.